

Temperature- and pH-Sensitive IPNs Grafted onto Polyurethane by Gamma Radiation for Antimicrobial Drug-Eluting Insertable Devices

Franklin Muñoz-Muñoz,¹ Emilio Bucio,² Beatriz Magariños,³ Angel Concheiro,⁴
Carmen Alvarez-Lorenzo⁴

¹Departamento de Físicoquímica de Nanomateriales, Centro de Nanociencias y Nanotecnología, Universidad Nacional Autónoma de México, Km. 107 Carretera Tijuana-Ensenada, Mexico

²Departamento de Química de Radiaciones y Radioquímica, Instituto de Ciencias Nucleares, Universidad Nacional Autónoma de México, Ciudad Universitaria, 04510 Mexico DF, Mexico

³Departamento de Microbiología y Parasitología, Facultad de Biología CIBUS, Universidad de Santiago de Compostela, 15782-Santiago de Compostela, Spain

⁴Departamento de Farmacia y Tecnología Farmacéutica, Facultad de Farmacia, Universidad de Santiago de Compostela, 15782-Santiago de Compostela, Spain

Correspondence to: F. Muñoz-Muñoz (E-mail: frankmm@cnyunam.mx)

ABSTRACT: Temperature- and pH-sensitive interpenetrating polymer networks (IPNs) and semi-interpenetrating polymer networks (s-IPNs) were γ -ray grafted onto polyurethane (Tecoflex[®]; TFX) to obtain vancomycin-eluting implantable medical devices with minimized risk of infections. N-isopropylacrylamide (NIPAAm) was grafted onto TFX catheters and films via a preirradiation oxidative method (method P) or via a direct method (method D). The PNIPAAm network facilitated acrylic acid (AAc) inclusion and subsequent polymerization/crosslinking, under specific reaction conditions. IPNs and s-IPNs systems were characterized regarding the amount of grafted polymers, surface properties (FTIR-ATR, ESEM, EDX), thermal behavior (DSC), and their temperature- and pH-responsiveness. Loading and release of vancomycin for preventing *in vitro* growth of *Staphylococcus aureus* were also evaluated. Antimicrobial activity tests and hemo- (hemolysis, protein adsorption, thrombogenicity) and cyto-compatibility (cell viability and production of cytokines and NO) assays indicated that the modification of TFX by γ -radiation may improve the performance of polyurethanes for biomedical applications. © 2013 Wiley Periodicals, Inc. *J. Appl. Polym. Sci.* **2014**, *131*, 39992.

KEYWORDS: irradiation; grafting; stimuli-sensitive polymers; drug delivery systems; biomedical applications

Received 24 August 2013; accepted 23 September 2013

DOI: 10.1002/app.39992

INTRODUCTION

Polyurethanes are widely used as implantable biomaterials for devices in the form of catheters, vascular grafts, tracheal tubes, sutures, colostomy and ileostomy bags, wound dressings, controlled drug delivery depots, etc.^{1–3} Nevertheless, polymers intended to remain in contact with human body for a long time have an inherent risk of local and bloodstream infections due to microbial adhesion and proliferation (biofilm formation), which are associated to significant morbidity and mortality.^{4–6} Moreover, recognition from the host as a foreign body may lead to adverse reactions in the form of inflammation and thrombus formation.^{7,8}

Polyurethanes can be functionalized at the surface or in the bulk with other molecules/polymers that possess certain functional groups, such as amides, amines, carboxylic acids or epoxy to improve the blood contacting reactions and the resistance to infection, by applying different methods.⁹ Condensation with hydroxyl- or amino-bearing monomers has been shown suitable for promoting physical adsorption of antimicrobial agents, such as amikacin and ceftazidime.⁹ Derivatization with one or more nitrogen-halogen-containing molecules, such as N-halamine, endowed polyurethane surfaces with bactericidal properties,¹⁰ while with quaternary ammonium groups allowed antiviral features.¹¹ Coating with hydrophilic polymers has been used to immobilize silver sulfadiazine.¹² Grafting of methacrylic acid

Additional Supporting Information may be found in the online version of this article.

The work described in this article is the subject of patent application P201231908 filed by the University of Santiago de Compostela and the Universidad Nacional Autónoma de México.

© 2013 Wiley Periodicals, Inc.

(MAAc) onto ozone activated polyurethane resulted useful for conjugation of chitosan that, in turn, adsorbed and regulated the release of rifampicin.¹³ Compared to the referred techniques, γ -ray grafting may be advantageous since it is applicable to a wide variety of shapes and polymer–monomer combinations, does not require chemical initiators, and thus renders functionalized biomaterials without remnant residues.^{14,15} However, γ -ray grafting has still been rarely applied to polyurethane modification.¹⁶

Recent reports have described the functionalization with smart (stimuli-responsive) polymers applying γ -radiation as a tool for preventing biofilm formation on biomedical devices and to achieve the coupling of antimicrobial, anti-inflammatory, or immunosuppressive agents.^{17–20} Stimuli-responsive polymers can be grafted or incorporated as part of interpenetrating polymer networks (IPNs) with at least one network previously covalent attached to the polymer matrix.^{21–24} In a sequential IPN, a second polymer network is polymerized within a prepolymerized network, while in a semi-IPN (s-IPN) a linear polymer is entrapped within the original network.²⁵ The final IPN retains the properties of each individual polymer, improving deficient characteristics or even achieving additional features. In our previous works, different IPNs containing pH-responsive poly(acrylic acid) (PAAc) and temperature-responsive poly(N-isopropylacrylamide) (PNIPAAm) were grafted onto polypropylene (PP) in order to obtain *net*-PP-*g*-PAAc-*inter*-*net*-PNIPAAm²¹ and *net*-PP-*g*-PNIPAAm-*inter*-*net*-PAAc^{22–24} by combination of both γ -radiation (for grafting reaction) and redox polymerization (for obtaining the second network). These materials were found to be capable of loading vancomycin and to sustain its release and, in turn, to inhibit the formation of methicillin resistant *Staphylococcus aureus* (MRSA) biofilms.²² This drug is one of the most frequently chosen antibiotics for the treatment of infections associated with the use of implantable device, particularly catheters.⁶

The aim of this work was to γ -ray graft temperature- and pH-responsive IPNs and s-IPNs systems containing PNIPAAm/PAAc onto two types of polymeric matrices both made of Tecoflex[®] (TFX), commercially available biomedical-grade polyurethane used for the manufacture of implantable devices, in order to endow the surface or the bulk with capability to load vancomycin and sustain its release. The final purpose is to avoid the risk of bacterial contamination upon medical insertion, while maintaining the original mechanical and biocompatibility properties. The effect of a number of variables (such as dose radiation, monomer concentration, solvents) on the grafting yield and structure was evaluated regarding the performance of the functionalized materials. Thus, three IPNs (*net*-TFX-*g*-PNIPAAm-*inter*-*net*-PAAc with PNIPAAm grafted onto the TFX surface; *net*-TFX-*g*-PNIPAAm-*inter*-*net*-PAAc with PNIPAAm grafted in the bulk matrix; and TFX-*g*-*net*-PNIPAAm-*inter*-*net*-PAAc with PNIPAAm grafted and crosslinked simultaneously in one step synthesis) and two s-IPNs systems (TFX-*g*-PNIPAAm-*inter*-*net*-PAAc with PNIPAAm grafted onto surface; and TFX-*g*-PNIPAAm-*inter*-*net*-PAAc with PNIPAAm grafted in the bulk) were synthesized and characterized regarding swelling responsiveness, *in vitro* hemo- and cyto-compatibility, inflammatory response and drug release performance.

EXPERIMENTAL

Materials

UMBILI-CATH[™], a single-lumen radiopaque umbilical catheter made with polyurethane Tecoflex[®] (TFX), with 1.67 mm (5 Fr) diameter, was provided by UTAH Medical Products. TFX catheters were cut into 2.5 cm long pieces, washed with methanol, toluene and ethanol for 24 h each, and then dried under vacuum at 40°C. Polyurethane TFX EG-93A films (TFX film) with 0.5 mm of thickness were provided by Lubrizol Advanced Materials, Thermedics Polymer Products. TFX film was cut into 1.0 cm × 4.0 cm pieces, washed and dried as TFX catheters. N-isopropylacrylamide (NIPAAm) and acrylic acid (AAc) were from Aldrich. NIPAAm was purified by recrystallization in hexane/toluene (50/50 vol. %) and AAc was vacuum distilled for purification. N,N'-metylenbisacrylamide (MBAAm) was used as supplied by Sigma-Aldrich. Boric acid, citric acid, ethanol, hexane, methanol, toluene, and trisodium orthophosphate were from JT Baker., México; bovine serum albumin (BSA) from Acros Organics., Belgium; fibrinogen, glacial acetic acid, sodium citrate and sodium hydroxide (NaOH) from Panreac Química S.A., Spain; ethylenediaminetetraacetic acid (EDTA), naphthol blue black and Physiological Buffer Solution (PBS pH 7.4) from Sigma-Aldrich Co., Spain; formaldehyde from Scharlab S.L., Spain; potassium phosphate monobasic (KH₂PO₄) from Merck., Germany, and vancomycin-HCl from Roig Farma., Spain; all were used as received. Nitrocellulose membrane filters with 8.0 μ m of pore size and 160 μ m of thickness were from Merck Millipore. Cytotoxicity Detection kit^{PLUS} [Lactate Dehydrogenase (LDH)] was from Roche, Spain. Distilled water was used for synthesis and characterization experiments, and ultrapure water with resistivity > 18.2 M Ω cm (Millipore Iberica, Spain) was utilized in antimicrobial activity tests and hemo- and cyto-compatibility assays. Phosphate buffer pH 7.4 contained 0.2M NaOH and 0.2M KH₂PO₄.

Grafting of PNIPAAm onto TFX Catheters and Films (TFX-*g*-PNIPAAm)

Preirradiation Oxidative (Method P). TFX pieces were irradiated in air at room temperature with ⁶⁰Co γ -sources (Gammabeam 651 PT; Nordion Co., Canada) at dose rate of 7.4 kGy/h and different radiation doses (from 2.5 to 50 kGy). The preirradiated TFX pieces (previously weighed) were placed in glass ampoules containing aqueous solutions of NIPAAm (0.5 or 1.0M; 8 mL). The ampoules were saturated with argon for 20 min, sealed and heated at 60 or 70°C for different times (from 45 to 420 min). The grafted polymers were repeatedly washed with water for 5 days (replacing the medium several times) and then dried at 40°C for 48 h. The weight percentage of the grafted material was calculated as:

$$g(\%) = \left[\frac{(W_f - W_i)}{W_i} \right] 100 \quad (1)$$

W_f and W_i being the weights of TFX pieces after and before grafting, respectively. TFX catheter was also irradiated in the absence of monomer to determine weight loss due to degradation.

Direct Irradiation (Method D). TFX pieces were weighed and placed in glass ampoules with solution of NIPAAm (0.5 or 1.0M; 9 mL) in toluene. The ampoules were saturated with

argon for 20 min, sealed and then irradiated at different doses (from 2.5 to 50 kGy), using dose rates of 2.9, 7.4 or 9.2 kGy/h. The grafted pieces were washed with toluene for 2 days and then with water for 7 days in order to extract the residual monomer, homopolymer or solvent. The grafted polymers were dried under vacuum. The grafting percentage was estimated using equation 1.

Crosslinking of the PNIPAAm Grafted onto TFX Catheters and Films (*net*-TFX-*g*-PNIPAAm)

TFX-*g*-PNIPAAm pieces prepared as described in method P and D were placed in glass ampoules with water (8 mL) and, after saturation with argon (20 min), sealed and then irradiated at a dose rate between 7.4 and 9.0 kGy/h at a radiation dose of 10 kGy. The crosslinked samples were immersed in water for 3 days and dried under vacuum at 40°C. The pieces were carefully washed to manually remove free homopolymer from the surface.

Grafting of *net*-PNIPAAm onto TFX Catheters (TFXcatheter-*g*-*net*-PNIPAAm)

TFXcatheter-*g*-*net*-PNIPAAm materials were prepared as in method P, at dose rates from 8.0 to 8.6 kGy/h, using doses between 10 and 50 kGy, and filling the ampoules with aqueous solutions of NIPAAm (0.25, 0.5 or 1.0M) containing MBAAm at different weight percentages (from 0.05 to 2.0 wt %). The grafted catheters were washed with water for 5 days and dried under reduce pressure.

Polymerization and Cross linking of AAc Interpenetrated Within TFX-*g*-PNIPAAm, *net*-TFX-*g*-PNIPAAm, and TFXcatheter-*g*-*net*-PNIPAAm

To obtain s-IPNs (TFX-*g*-PNIPAAm-*inter*-*net*-PAAc) or IPNs (*net*-TFX-*g*-PNIPAAm-*inter*-*net*-PAAc or TFXcatheter-*g*-*net*-PNIPAAm-*inter*-*net*-PAAc), polymerization, and crosslinking of AAc stimulated by γ -radiation was carried out inside the materials prepared as described in all previous sections. Each sample (previously weighed) was placed in glass ampoules that contained aqueous solutions of AAc 25 % v/v with MBAAm 1 % w/w (8 mL). After 6 h the monomer solution was removed, and the swollen pieces were frozen in liquid nitrogen and simultaneously degassed by vacuum for 15 min. The ampoules were sealed and immediately irradiated at dose of 1.5 kGy and dose rate 5 kGy/h. The products obtained were then washed with water for 7 days (removing excess gel manually) and dried at 40°C under vacuum. Triplicate samples were prepared for each NIPAAm/AAc composition and grafting degree. The amount of PAAc into the s-IPN or IPNs was evaluated by weighing the samples before and after PAAc polymerization.

Characterization of the Grafted Polymers

Infrared Analysis. FTIR-ATR (attenuated total reflection) spectra were recorded from 650 to 4000 cm^{-1} using a Perkin-Elmer Spectrum 100 (Perkin Elmer Cetus Instruments, Norwalk CT) equipped with a Universal ATR sampling accessory and a diamond tip. Baseline subtraction was carried out using the Spectrum software supplied with the equipment.

Environmental Scanning Electron Microscopy (ESEM) Imaging. Unmodified and modified TFX catheters previously swollen in phosphate buffer pH 7.4, were observed using an EVO LS₁₅

ESEM under 500x magnification, on cryogenically fractured tubing in transverse directions, at temperature and pressure variables (7°C – 650 Pa and 35°C – 10 Pa), using Backscattered Electron Detector (BSE). Qualitative and semiquantitative elemental chemical composition of the unmodified TFX (film and catheter) was determined by Energy-dispersive X-ray spectroscopy (EDXS) (resolution 129 eV and WD 8.5). EDX analysis was performed to gain information regarding both elemental quantification and distribution/mapping of the components.

Differential Scanning Calorimetry. DSC scans were recorded using at 10°C/min, from 30 to 300°C under nitrogen atmosphere (60 mL/min) (TA Instruments 2010; New Castle DE).

Swelling Behaviour. Dried polymers were immersed in buffer solution pH 7.0 at 25°C and weighed at different times (after wiping the surface with a soft tissue). The swelling degree was calculated as:

$$S_w(\%) = 100 [(W_t - W_i) / W_i] \quad (2)$$

W_t and W_i being the weights of the swollen polymer at time t and of the dry polymer, respectively. The ratio of the swelling degree at 10 and 50°C was used to quantify the temperature-responsiveness, as follows:

$$S_T = S_{ST} / S_{CT} \quad (3)$$

In this equation, S_{ST} is the highest swelling (swollen state) and S_{CT} is the lowest swelling (collapsed state) in the temperature range studied. The “lower critical solution temperature” (LCST) was estimated as the inflection point of the S_w (%) vs. temperature plot.

The sensitiveness to pH was evaluated at 25°C by immersion universal buffer of pH range 2–11 was prepared by mixing a stock solution of 0.2M boric acid and 0.05M citric acid with a second stock solution of 0.1M trisodium orthophosphate solutions.²⁶ pH values were determined in HI 4212 potentiometer Hanna Instruments, CA. The responsiveness was quantified as the ratio of the highest (S_{SpH}) to the lowest swelling (S_{CpH}) values:

$$S_{pH} = S_{SpH} / S_{CpH} \quad (4)$$

The critical pH was identified as the inflection point of the S_w (%) vs. pH plot.

Vancomycin Loading/Release and Antimicrobial Activity Test

The IPNs and s-IPNs were immersed in pH 8.0 buffer at 5°C for 24 h. Some polymers were dried at 40°C while others were used in swollen state. The samples were placed in vancomycin aqueous solution (0.4 mg/mL, 5 mL) at 5°C for 80 h protected from light and the amount of drug loaded was calculated from the difference between the initial and the final concentration by UV spectrophotometry at 280 nm (Varian Cary 100 UV-vis spectrophotometer, Palo Alto, CA). Some pieces (18–25 mg) were dried at 40°C and others were kept in swollen state and then transferred to test tubes containing 5 mL of phosphate buffer pH 7.4 (ionic strength 0.27) at 37°C. The release experiments were carried out in triplicate under *sink* conditions and

without stirring and the amount of vancomycin released was monitored spectrophotometrically at 280 nm for 48 h.

The Kirby–Bauer method²⁷ was used for antimicrobial activity testing of IPNs and s-IPNs films (disks diameter 9 mm) and catheters (long 1 cm) previously sterilized (121°C, 20 min) and loaded by immersion in vancomycin solutions (previously filtered through 0.22 μm membranes) as described above. After 80 h the amount adsorbed on the polymers was quantified. Drug-loaded pieces were placed on a Mueller–Hinton agar plate (MH agar medium, OXOID, England) seeded with *Staphylococcus aureus* (ATCC 25923). The plates were incubated at 37°C for 24 h. This procedure was also applied to unloaded polymers. Samples were tested in duplicate. Following incubation, the plates were examined for zones of inhibition around the TFX disks or tubing.

Protein Adsorption

Unmodified and modified TFX films, previously washed three times with water and phosphate buffer solution pH 7.4, were cut into 9 mm diameter pieces and placed into separate test tubes (2 mL LoBind Eppendorf). Nitrocellulose disks (9 mm diameter pieces) were used as positive controls, while empty test tubes acted as negative controls. Solutions of 600 μL of 3 mg/mL fibrinogen or 30 mg/mL BSA were added onto each test and control samples, and then were incubated for 1 h at 37°C. The tubes were rinsed two times with water and subsequently immersed for 3 min in the staining solution which contained 45 mL each of methanol and water, 10 mL glacial acetic acid, and 100 mg of naphthol blue black.^{28,29} Following staining, the samples were rinsed three times with wash solution containing 90 % methanol, 8 % water, and 2 % glacial acetic acid, and then rinsed two times with water. Eluent solution (600 μL) composed of 50 % ethanol and 50 % 50 mM NaOH with 0.1 mM EDTA was added in all the tubes and then were agitated at 37°C for 30 min at 300 rpm and centrifuged at 3000g for 3 min at room temperature for removing the dye bound to the surface. Aliquots (100 μL) from the resulting solutions were transferred to a 96-well plate and the absorbance measured at 595 nm in FLUOstar OPTIMA reader (BMG Labtech). Duplicate samples were used for test and a standard curve of known concentrations of protein solution was used to calculate the amount of protein adsorbed to each surface. Triplicate samples of nitrocellulose disks were used for the positive control tests.

Hemolysis

Blood from Sprague–Dawley rats was kept with sodium citrate solution (3.8 wt %) in a 9:1 ratio and used within the first 24 h. Unmodified and modified catheters were cut into small pieces (1 cm long), swollen in phosphate buffer pH 7.4 for 24 h, and then placed in plastic tubes containing 5 mL of PBS buffer. Rat blood (0.25 mL) was added and all tubes were incubated for 60 min at 37°C and then centrifuged at 700g for 10 min. The hemolysis was determined by recording the absorbance of the plasma supernatants at 542 nm in a UV-vis spectrophotometer (Agilent 8453, Germany). Positive and negative controls were obtained by adding 0.25 mL diluted blood to 5 mL water and PBS buffer, respectively. Less than 5% hemolysis

was regarded as the permissible level. The assay was performed in duplicate.

Thrombogenicity

Native and modified films (1 \times 1 cm) were swollen in phosphate buffer pH 7.4 at 37°C for 2 h and then placed on Petri dishes. Sprague–Dawley rat blood (0.1 mL with sodium citrate) was added onto each film. Blood clotting was initiated by adding 0.01 mL of 0.1 M CaCl_2 solution on the surface covered by the blood solution.³⁰ After 30 min, the reaction was stopped by adding water (2.5 mL). Clot formed was recovered from the films with a spatula and fixed in 37 % formaldehyde aqueous solution (5 mL). The fixed clots were dried under vacuum at room temperature and weighed. Positive controls were similarly carried out but on an empty glass Petri dish to which the blood was directly added. The experiments were carried out in duplicate.

Cytocompatibility

RAW 264.7 cells were seeded (1×10^5 , 2 mL) on 24 well tissue culture polystyrene plates to which UV-sterilized and swollen TFX film (IPNs) pieces were added. Aliquots (500 μL) from the culture medium were collected after 24 and 72 hours of incubation and immediately frozen at -20°C ; the aliquot was replaced with 500 μL of fresh medium. The experiments were carried out in duplicate for each film and data point. Negative (cells in culture medium without sample) and positive [cells in culture medium with 1 $\mu\text{g}/\text{mL}$ of lipopolysaccharide, (LPS)] controls were processed in parallel. Cytotoxicity was evaluated using the LDH Cytotoxicity Detection kit^{PLUS}; absorbance at 490 nm was measured using a plate reader (Bio-Rad 680).

NO production was assayed by measuring the nitrate of supernatants at 24 and 72 hours. Aliquots (80 μL) of culture supernatants were mixed with 100 μL of the Griess reagent^{31,32} and after 10 minutes of incubation at room temperature the plates were read at 550 nm. NO concentration was quantified by means of a calibration curve of sodium nitrate (0–15 μM).

TNF- α levels in the supernatants were quantified by means of ELISA (Bender MedSystems GmbH, Austria), reading the absorbance at 450 nm, as previously reported.¹⁹

RESULTS AND DISCUSSION

TFX (Figure 1) is a cycloaliphatic poly(etherurethane) synthesized from 4,4'-methylenedicyclohexyl diisocyanate (H_{12}MDI), 1,4-butanediol (BD) and poly(tetramethylene glycol) (PTMG).³³ The surface elemental composition of both polyurethanes TFX and radiopaque portion in TFX catheter is shown in Supporting Information Table SI. The composition of all functionalized polymers, from the grafting step until preparation of the corresponding s-IPN or IPN is shown in Table I. Each PNIPAAm graft level led to three types of functionalized materials: (i) TFX-g-PNIPAAm, designed as “GxP” or “GxD” where G indicates grafted, x is the PNIPAAm grafting percentage, and P or D indicates the grafting process by method P or D; (ii) net-TFX-g-PNIPAAm, designed as “CxP” or “CxD” where C indicates crosslinked; (iii) TFX-g-PNIPAAm-inter-net-PAAC, designed as

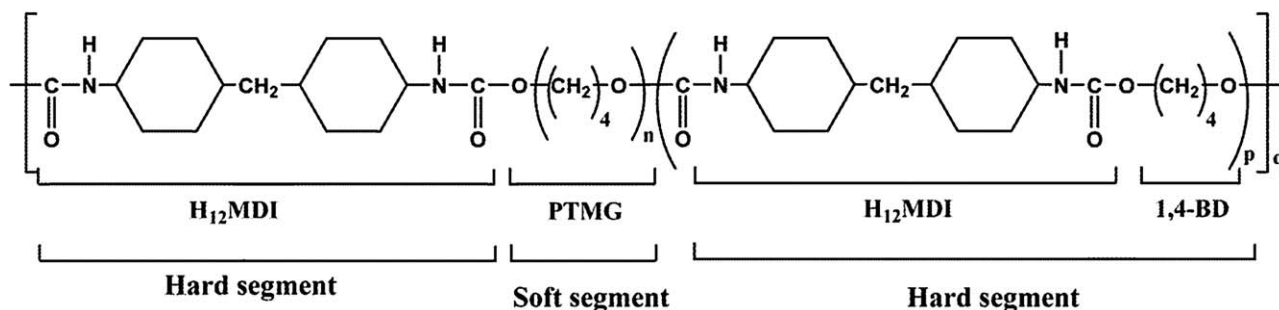


Figure 1. TFX structure.

“*s-IPNxP*” or “*s-IPNxD*”; and (iv) *net-TFX-g-PNIPAAm-inter-net-PAAc*, designed as “*IPNxP*” or “*IPNxD*” where *x*, *P* and *D* have the same meaning as above.

Preparation of the Grafted TFX

Method P. Preirradiation oxidative processed TFX catheters and films showed uni-axially changes in their dimensions (i.e., only in

Table I. Composition of TFX Polymers Modified with PNIPAAm/PAAc

| Catheter Code | PNIPAAm grafted g (%) | net-PAAc interpenetrated | | Film Code | PNIPAAm grafted g (%) | net-PAAc interpenetrated | |
|---------------|-----------------------|--------------------------------|------------------|------------|-----------------------|--------------------------------|------------------|
| | | PNIPAAm/PAAc ratio (% mol/mol) | TFXc-g-IPN g (%) | | | PNIPAAm/PAAc ratio (% mol/mol) | TFXf-g-IPN g (%) |
| GCc-1step | 19 (±0.7) | - | - | | | | |
| IPNc-2steps | 20 (±0.8) | 17/83 (±0.5) | 66.7 (±0.5) | | | | |
| G40P-c | 40 (±1.4) | - | - | G40P-f | 41 (±2.0) | - | - |
| C40P-c | 38 (±2.0) | - | - | C40P-f | 37 (±3.4) | - | - |
| IPN40P-c | 43 (±1.0) | 32/68 (±1.1) | 96 (±3.2) | IPN40P-f | 43 (±3.6) | 26/74 (±1.5) | 119 (±1.1) |
| s-IPN40P-c | 40 (±1.4) | 28/72 (±1.3) | 106 (±3.4) | s-IPN40P-f | 42 (±4.0) | 25/75 (±1.1) | 123 (±6.4) |
| G60P-c | 63 (±1.6) | - | - | G60P-f | 61 (±1.6) | - | - |
| C60P-c | 58 (±0.5) | - | - | C60P-f | 62 (±2.4) | - | - |
| IPN60P-c | 63 (±1.3) | 35/65 (±1.0) | 131 (±4.7) | IPN60P-f | 62 (±2.2) | 33/67 (±3.0) | 147 (±3.8) |
| s-IPN60P-c | 59 (±3.8) | 30/70 (±1.3) | 139 (±6.1) | s-IPN60P-f | 61 (±3.2) | 30/70 (±1.2) | 158 (±9.1) |
| G80P-c | 82 (±2.4) | - | - | G80P-f | 81 (±1.3) | - | - |
| C80P-c | 79 (±5.0) | - | - | C80P-f | 82 (±1.4) | - | - |
| IPN80P-c | 82 (±5.5) | 34/66 (±4.4) | 183 (±6.1) | IPN80P-f | 82 (±2.0) | 34/66 (±3.7) | 175 (±8.4) |
| s-IPN80P-c | 77 (±6.0) | 37/63 (±4.0) | 162 (±2.2) | s-IPN80P-f | 79 (±1.2) | 36/64 (±2.9) | 162 (±6.5) |
| G40D-c | 41 (±0.9) | - | - | G40D-f | 41 (±3.3) | - | - |
| C40D-c | 40 (±1.6) | - | - | C40D-f | 37 (±4.0) | - | - |
| IPN40D-c | 40 (±0.9) | 24/76 (±0.6) | 111 (±3.7) | IPN40D-f | 38 (±1.7) | 22/78 (±1.8) | 102 (±1.8) |
| s-IPN40D-c | 40 (±2.2) | 24/76 (±0.2) | 115 (±4.3) | s-IPN40D-f | 37 (±1.2) | 21/79 (±0.1) | 103 (±3.0) |
| G60D-c | 59 (±0.7) | - | - | G60D-f | 63 (±1.3) | - | - |
| C60D-c | 60 (±1.1) | - | - | C60D-f | 65 (±0.7) | - | - |
| IPN60D-c | 62 (±2.7) | 30/70 (±0.5) | 148 (±2.3) | IPN60D-f | 65 (±0.2) | 31/69 (±1.1) | 156 (±5.7) |
| s-IPN60D-c | 59 (±1.0) | 29/71 (±0.2) | 149 (±2.8) | s-IPN60D-f | 64 (±1.6) | 30/70 (±2.9) | 160 (±1.4) |
| G80D-c | 79 (±1.1) | - | - | G80D-f | 77 (±1.6) | - | - |
| C80D-c | 79 (±1.4) | - | - | C80D-f | 80 (±1.9) | - | - |
| IPN80D-c | 81 (±2.1) | 33/67 (±0.6) | 170 (±4.1) | IPN80D-f | 79 (±3.1) | 35/65 (±1.3) | 164 (±6.8) |
| s-IPN80D-c | 80 (±1.5) | 32/68 (±1.2) | 180 (±0.1) | s-IPN80D-f | 75 (±2.2) | 35/65 (±2.2) | 169 (±6.5) |

TFX-g-PNIPAAm is represented by G_x with “x” being the grafting percentage; C_x refers to *net-TFX-g-PNIPAAm* where “x” is the grafting percentage. “P” and “D” indicate the grafting method used. IPNs and s-IPNs represent *net-TFX-g-PNIPAAm-inter-net-PAAc* and *TFX-g-PNIPAAm-inter-net-PAAc*, respectively, and their complements refer to the corresponding grafting process. TFXc-g-*net-PNIPAAm* is represented by GC-1step, indicating that the grafting and crosslinking process occurred simultaneously, and its corresponding TFXc-g-*net-PNIPAAm-inter-net-PAAc* is represented by IPNc-2steps. Catheters and films are indicated by “-c” and “-f”, respectively.

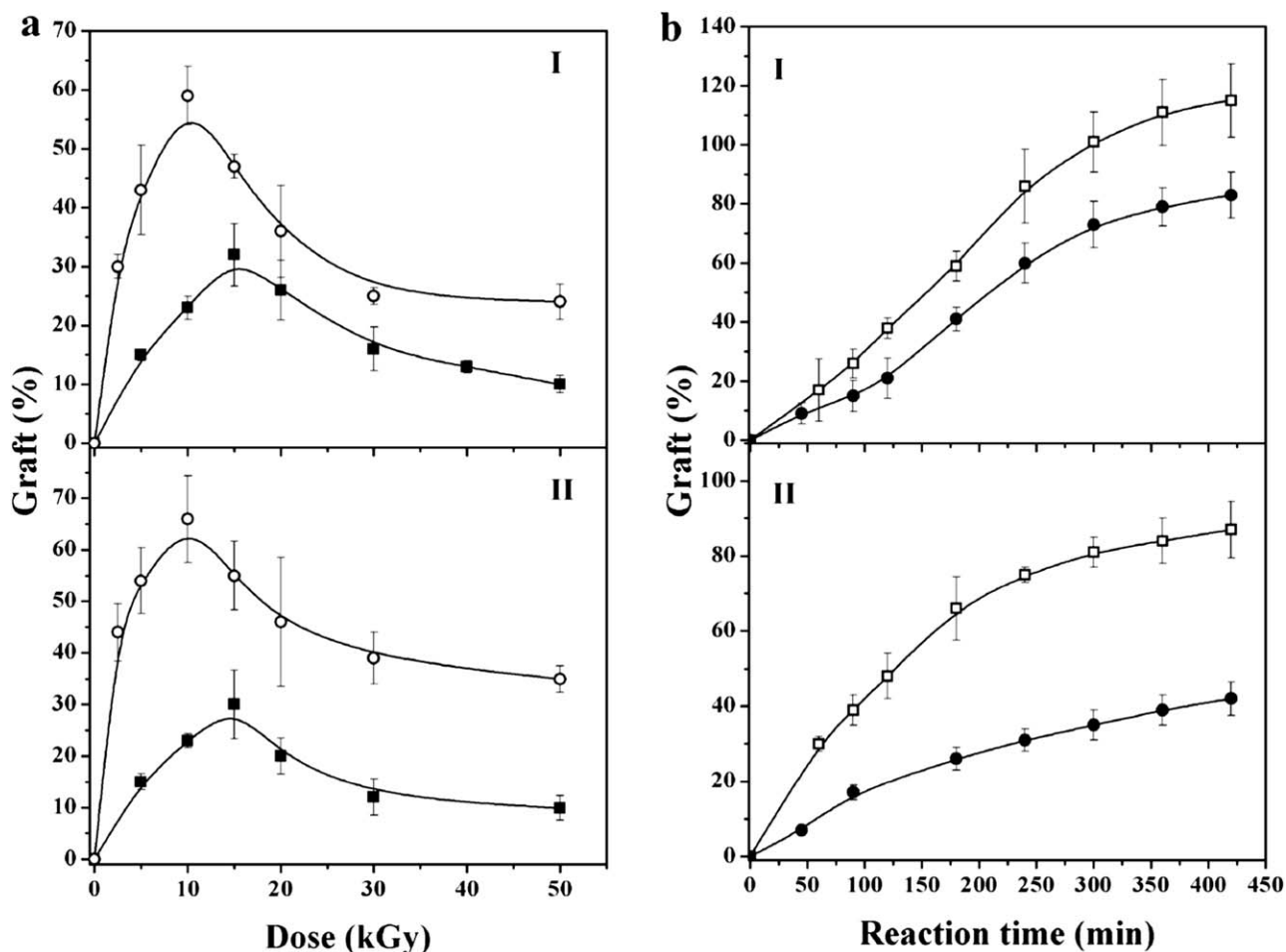


Figure 2. Grafting of PNIPAAm onto TFX catheter (I) and TFX film (II) by method P as a function of (a) radiation dose, at 70°C and a reaction time of 3 h, for two NIPAAm aqueous solutions: 0.5M (■) and 1M (○); and (b) reaction time, at a preirradiation dose of 10 kGy and 1.0M NIPAAm aqueous solution, for two temperatures: 60°C (●) and 70°C (□) (mean values and standard deviations). Dose rate of 7.4 kGy/h was applied in all experiments.

the diameter and the thickness, respectively) upon grafting of PNIPAAm, which indicates that the modification occurred at the surface. The amount of PNIPAAm grafted first increased as a function of radiation dose and a maximum was reached at 15 kGy for 0.5M or at 10 kGy for 1.0M and then decreased [Figure 2(a)]. The initial positive slope and the maximum grafting dose are explained considering that more radicals are created and can participate in the reaction when the dose and monomer concentration are increased. However, homopolymerization is predominant at high radiation doses as the amount of radicals formed is greater. This causes an increase in the viscosity of the grafting and makes the diffusion of NIPAAm onto TFX surface difficult. Under these reaction conditions, the radical recombination among the chains of the polymeric substrate can be promoted and the graft yield reduced. On the other hand, a high concentration of monomer increases the diffusion gradient on the polymer surface, resulting in a higher grafting degree at a lower dose. Therefore, preirradiation dose of 10 kGy and 1.0M NIPAAm were chosen in order to synthesize TFX-g-PNIPAAm. Monomer concentration above 1.0M was discarded because it produces high amounts of homopolymer, makes the extraction of the polymer difficult and increases the costs of the processing.

The amount of grafted PNIPAAm increased with increasing reaction time and temperature [Figure 2(b)], as observed for other polymers.³⁴ It is interesting to note that using relatively low preirradiation dose (10 kGy) and reaction times (1–4 h), high grafting yield can be attained. Grafting levels of roughly 40, 60, and 80% (w/w) were chosen for further studies because below 40% no thermosensitivity was observed whereas above 80% thickness and stiffness of the material were greatly increased.

Method D. Grafting of PNIPAAm on TFX was also carried out applying a direct method, that is, the catheters and films were irradiated while immersed in a solution of NIPAAm in the absence of oxygen, using toluene as a solvent which produces high swelling in polyurethanes (300–500 %). After grafting, the pieces exhibited a gradual increase of their thickness and also an expansion between the two in-plane dimensions (length and diameter for catheters, and length and width for films), which indicated that grafting occurred in the bulk matrix. Once again, the grafting percentages values were higher for 1.0M than for 0.5M monomer concentration (Figure 3) due to an increase in the diffusion and reactivity of the NIPAAm onto the polymer

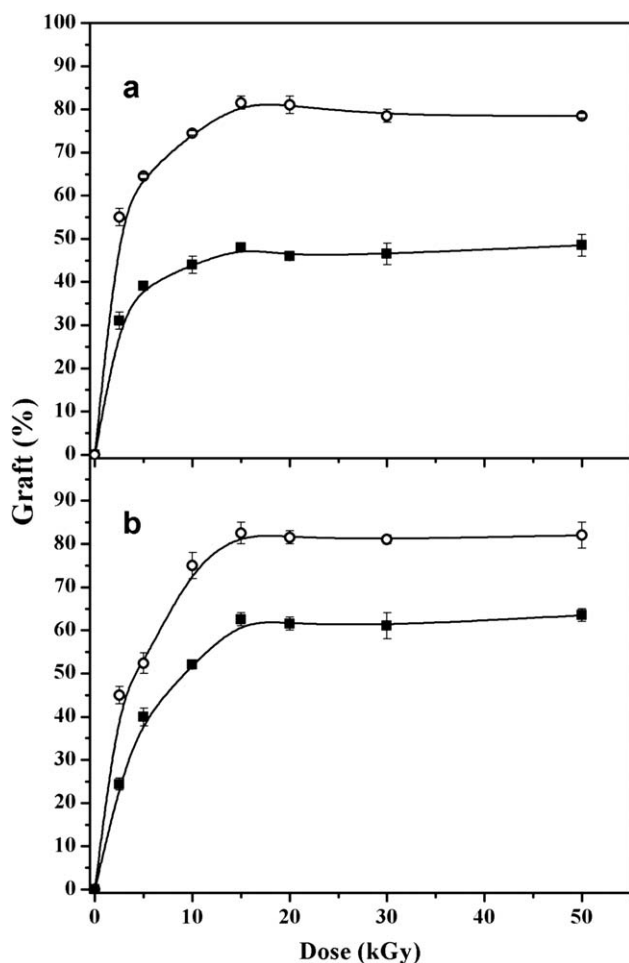


Figure 3. Grafting of PNIPAAm onto TFX catheter (a) and TFX film (b) by method D as a function of radiation dose for two NIPAAm solutions in toluene: 0.5M (■) and 1M (○) (mean values and standard deviations). Dose rate 7.4 kGy/h.

matrix. For both TFX catheters and films, the grafting yield attained a plateau above 15 kGy. For comparative purposes, the grafting levels selected were the same as those described in method P (roughly 40, 60, and 80 %; obtained at 5 kGy for 0.5M NIPAAm, and at 5 and 15 kGy for 1.0M NIPAAm, respectively).

Crosslinking of the TFX-g-PNIPAAm systems obtained via method P or D to prepare *net*-TFX-g-PNIPAAm was carried out in aqueous medium at 10 kGy (polymers denoted with “C” in Table I).

Grafting of *net*-PNIPAAm onto TFX Catheter (TFXcatheter-g-*net*-PNIPAAm)

Simultaneous grafting and crosslinking of PNIPAAm onto TFX catheter was carried out using the preirradiation oxidative method with the addition of MBAAm as a crosslinking agent. The amount of MBAAm chosen was 0.7 % w/w (0.05M) as in previous studies.^{22–24} The *net*-NIPAAm grafting process exhibited a similar trend to that described for the synthesis of TFX-g-PNIPAAm by method P [Figure 4(a)]. The maximum grafting percentage was reached at 20, 30, and 40 kGy for 1.0, 0.5, and

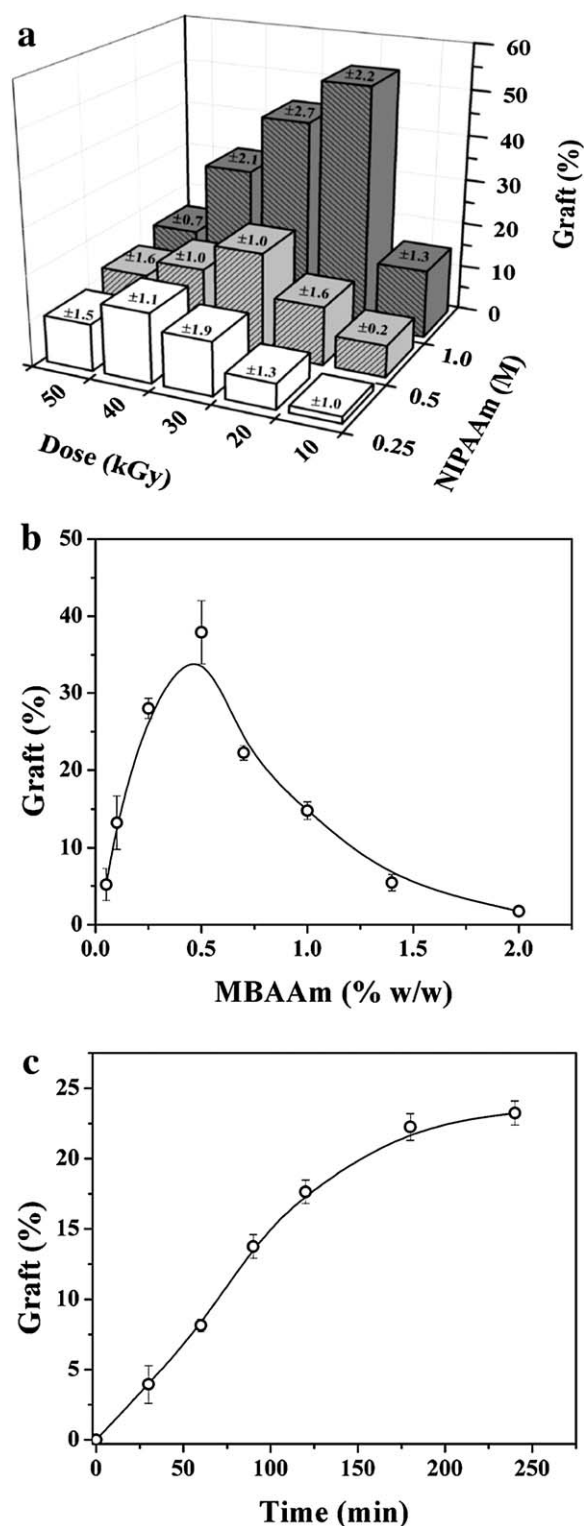


Figure 4. Grafting percentages of *net*-PNIPAAm onto TFX catheter in one step by preirradiation oxidative method as a function of (a) radiation dose at MBAAm 0.7 % w/w (0.05M), reaction time of 3h, and for three NIPAAm aqueous solutions: 0.25, 0.5, and 1M; (b) MBAAm concentration at a radiation dose of 30 kGy, reaction time of 3 h and 0.5M NIPAAm_{aq}; and (c) reaction time at NIPAAm/MBAAm concentration of 0.5/0.05M in aqueous solution. A rate dose of 8.3 kGy/h and a temperature of 70°C were applied in all experiments.

0.25M NIPAAm, respectively. Materials functionalized in the presence of 1M NIPAAm showed a rough and rigid surface (with restricted water permeability), while in the presence of 0.25M NIPAAm the surface modification was low. Under any of these two conditions, the grafted materials showed no temperature sensitiveness.

Total percentage grafting of the *net*-PNIPAAm in one step was tuned varying the MBAAm concentration from 0.05 to 2 % while keeping the irradiation dose, monomer concentration, reaction time and temperature constant [Figure 4(b)]. The surface of the TFXcatheter-*g-net*-PNIPAAm with <0.7 % MBAAm showed greater roughness, lower flexibility and less uniformity on the surface. Above 0.7 % MBAAm the amount of *net*-PNIPAAm grafted was low and unresponsive to temperature changes, with predominance of homopolymerization. Crosslinking agent concentration of 0.7% was chosen as optimal value. Grafting of *net*-PNIPAAm was greater to 70°C than at 80°C because the radical recombination reactions are promoted under at high temperature. Figure 4(c) shows the relationship between the *net*-PNIPAAm grafting levels and reaction time. About 20% grafting degree was chosen for further studies since above 25% an increase in rigidity and roughness occurred. The TFXcatheter-*g-net*-PNIPAAm was named as *GCC-1step* and its corresponding IPN as *IPNC-2steps* (Table I).

Polymerization and Crosslinking of AAc Interpenetrated within TFX-*g*-PNIPAAm, *net*-TFX-*g*-PNIPAAm, and TFXcatheter-*g-net*-PNIPAAm

First, direct irradiation of TFXcatheter in the presence of AAc aqueous solutions (radiation dose from 0.5 to 3.0 kGy) was carried out in order to identify a low dose capable of rendering PAAc networks (hydrogels) without leading to graft reactions between PAAc and TFX. A radiation dose of 1.5 kGy and a small proportion of crosslinker MBAAm were chosen as adequate for polymerization/crosslinking of the interpenetrating of PAAc network. The crosslinker helps to diminish the radiation dose necessary to form the PAAc network, thus reducing the graft reactions between the monomer and the polyurethane matrix.

All steps followed for the synthesis of *Gx*, *Cx*, and *GCC-1step*, and the subsequent interpenetration of the PAAc network are depicted in Figure 5. Generally, the higher the PNIPAAm grafting percentage, the greater the amount of IPN grafted onto or in TFX (i.e., more PAAc can be interpenetrated in the PNIPAAm chains or network) (Table I). IPNs and *s*-IPNs with 40% grafting, synthesized by method D, had PNIPAAm:PAAc ~20:80 mol/mol ratio while all other polymers had ~30:70 mol/mol ratio. Short chains grafted on the polymer bulk also act as spacers among TFX chains, thus favoring the entry of more AAc before its polymerization into the matrix.

Characterization of the Grafted Polymers

Functionalization of TFX catheters and films was confirmed by the appearance of new bands of carboxylic acid, amide and isopropyl groups in the FTIR spectra (Supporting Information Figure S1). The native TFX presents characteristic bands at 3316 (NH stretching), 2920–2796 (asymmetric and symmetric CH₂

stretching from polyether and cyclohexane), 1714–1693 (C=O stretching from amide I group), 1525 (C–N stretching + N–H bending from amide II band), 1228 (C–N stretching from amide III band), 1097 (asymmetric C–O–C stretching from polyether), 1044 (asymmetric C–O–C stretching from urethane region), 980 (asymmetric ring stretching from cyclohexane) and 780 cm⁻¹ (cyclohexane ring breathing).^{35–37} The grafting of PNIPAAm via preirradiation method (*G60P*) was evidenced by the appearance of bands at 3289, 1635, and 1537 cm⁻¹, which confirmed the presence of amide group, and a doublet at 1386 and 1367 cm⁻¹ assigned to the isopropyl group;³⁸ the reduction or disappearance of the characteristic bands of TFX (1714, 1693, 1228, and 780 cm⁻¹) indicated that PNIPAAm was mainly grafted onto the polymer surface. The grafting process via direct method (*G60D*) was evidenced by the appearance of characteristic bands of PNIPAAm, while preserving the characteristic bands of TFX; this indicates that the direct irradiation led to the bulk modification of the matrix. No differences were observed between TFX-*g*-PNIPAAm and the crosslinked counterparts, which confirmed that the crosslinking was essentially intramolecular, no intermolecular, without affecting other chemical groups.²³ The *s*-IPNs and IPNs showed an increase in the intensity of the overlapping bands of the carboxylic (1715 cm⁻¹) and hydroxyl (3300 cm⁻¹) groups of PAAc. No differences were observed between TFX catheter [Supporting Information Figure S1(a)] and film [Supporting Information Figure S1(b)] materials, which confirmed that the functionalization occurred in the same way independently of the shape and manufacturing characteristics of the polyurethane matrix. The functionalization of TFX catheter with NIPAAm/AAc was also carried out on the radiopaque region of the catheter and the grafting was evidenced by the appearance of characteristic bands of PNIPAAm and PAAc.

The grafting of *net*-PNIPAAm onto TFX catheter by one-step and the formation of its corresponding IPN was evidenced by the appearance of new bands assigned to PNIPAAm (amide and isopropyl groups) and PAAc (non-ionized and ionized carboxylic acid groups).³⁹ Reduction or disappearance of the characteristic bands of TFX catheter, after functionalization, indicated that the modification mainly occurred on the polymer surface.

E-SEM micrographs of crosscut views of native and functionalized TFX catheter with different grafting PNIPAAm methods are shown in Supporting Information Figure S2. A spongy and thin layer of PNIPAAm covering the TFX catheter surface was observed in all polymers functionalized via the preirradiation oxidative method (*GCC-1step*, *G60P-c*, and *C60P-c*). The surface of *GCC-1step* showed many protuberances and greater roughness. The polymer materials grafted with PNIPAAm by method D did not show changes on the surface, but changes in the matrix were evident. Interpenetration of the second PAAc network (*net*-PAAc) into the first PNIPAAm network (*GCC-1step*, *C60P-c*, and *C60D-c*) or into the PNIPAAm chains grafted (*G60P-c* or *G60D-c*) affected the characteristics of both the surface and the bulk. The radiopaque polymer segments were affected in the same way as in the transparent areas (data not shown).

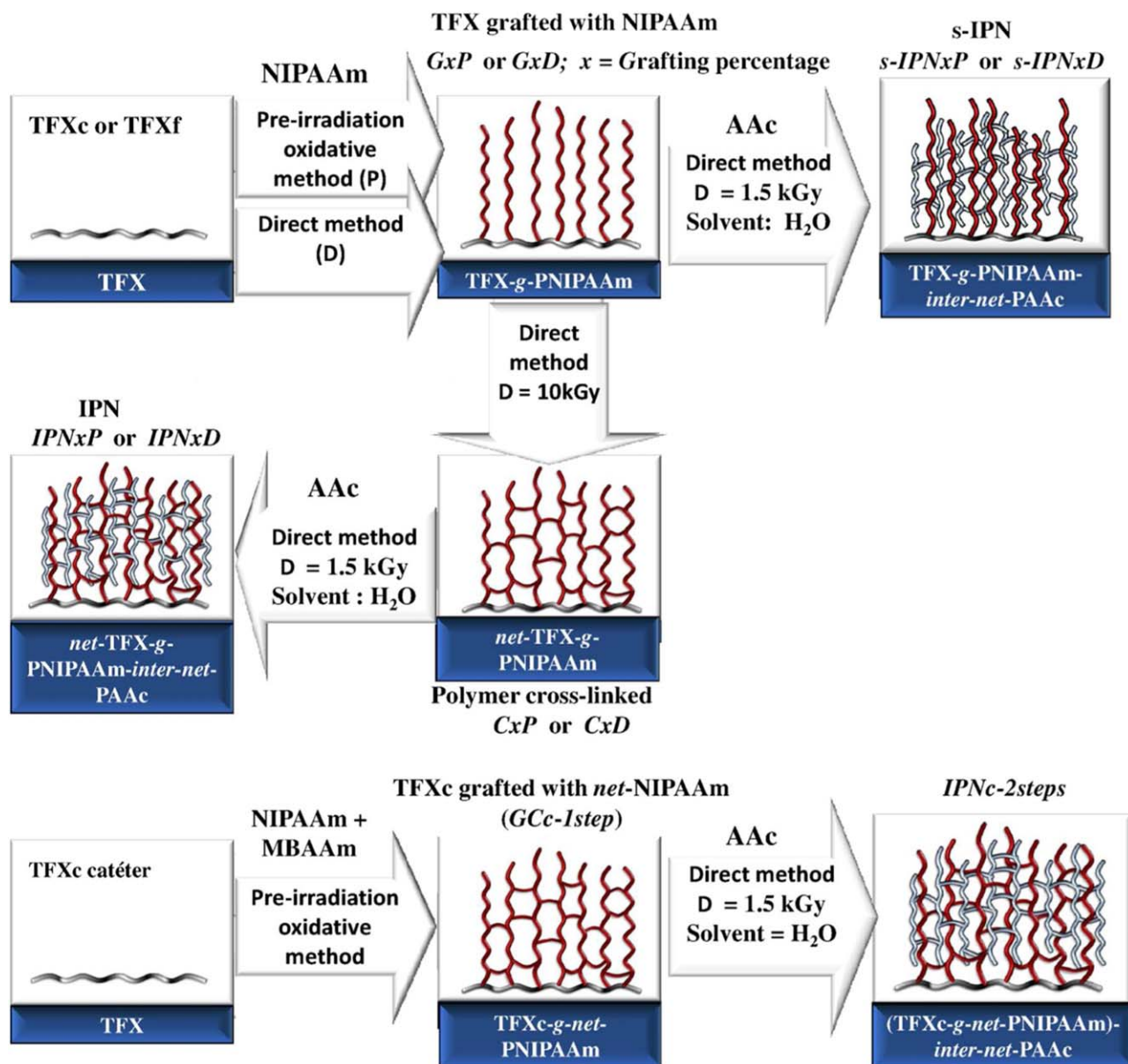


Figure 5. Polymerization steps followed to graft NIPAAm brushes and networks and NIPAAm/AAC IPNs and semi-IPNs to TFX films and catheters. [Color figure can be viewed in the online issue, which is available at wileyonlinelibrary.com.]

DSC scans evidenced the characteristic glass transition temperature (T_g) and melting point (T_m) of TFX catheter and film at 88, 134°C and 102, 126°C, respectively (Supporting Information Figure S3). The differences between the two types of TFX studied lies in the degree of phase mixing. The endotherm observed between 80 and 100°C for TFX catheter can be assigned to the disruption of short range order of hard segments microdomains, while the transition at 120–134°C can be due to the disruption of long-range and microcrystalline order of the hard segments.⁴⁰ In *GcC-1step*, the T_g of TFX catheter was not clearly observed while its T_m was preserved at 132°C [Supporting Information Figure S3(a)]. The second order transition (T_g) of PNIPAAm was not seen. The appearance of a T_g depends on the mobility of the polymer chains.⁴¹ T_g were not observed for the IPNc-2steps, but T_m was shifted toward a higher tempera-

ture (144°C), indicating that the PAAC units may be able to get incorporated into the mixing phase to reinforce the crystalline domains of TFX catheter. T_g of PNIPAAm chains for TFXcatheter-g-PNIPAAm (*G60P-c*) and *net-TFXcatheter-g-PNIPAAm* (*C60P-c*), both grafted by method P, was seen at 107 and 111°C, respectively [Supporting Information Figure S3(b)]. These values are consistent with those reported for PNIPAAm, in the range of 85–130°C.²² The glass transition temperature increases with increasing crosslinking density of the polymer, since the segmental mobility decreases.⁴² T_m was not significantly shifted toward higher temperatures for the *IPN60P-c* and *s-IPN60P-c*, demonstrating that PAAC was incorporated preferably in between the PNIPAAm chains (onto surface) and to a lesser extent on the crystalline arrangements (in the bulk matrix).

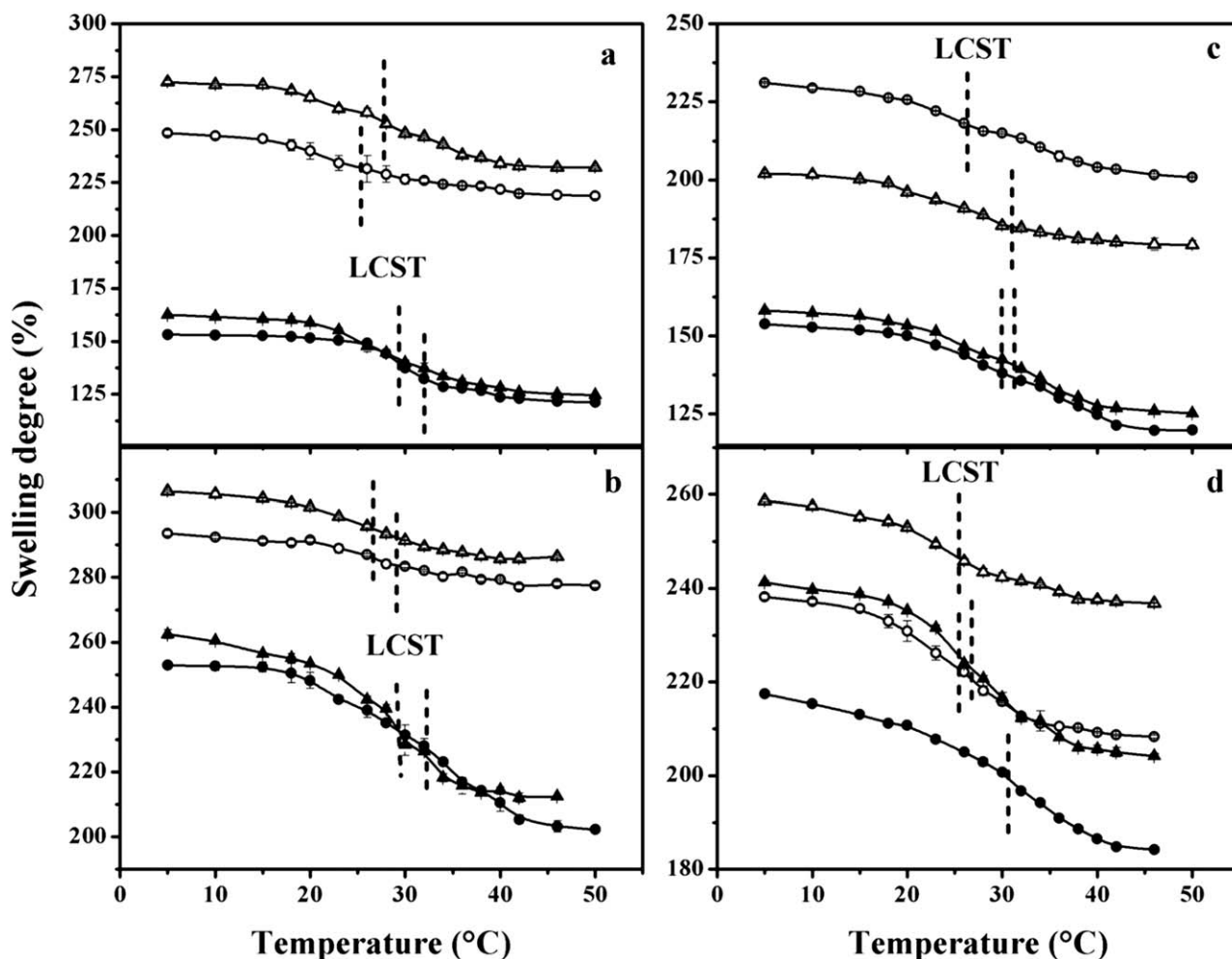


Figure 6. Swelling degree as a function of temperature in buffer solution pH 7.0 of TFX-*g*-PNIPAAm-*inter-net*-PAAc and *net*-TFX-*g*-PNIPAAm-*inter-net*-PAAc with PNIPAAm grafted by method P on catheters (a) and on films (c); and those with PNIPAAm grafted by method D on catheters (b) and films (d) for IPN40 (●), *s*-IPN40 (○), IPN60 (▲) and *s*-IPN60 (△). The dashed line represents the critical points.

T_g was observed only for the PNIPAAm grafted by direct irradiation (*G60D-c*) and not for crosslinked systems. Crosslinking of PNIPAAm chains reduced its mobility and T_g was not detected due to the restricted motion of chains segments near crosslinking sites (as in *C60D-c*). T_m was not significantly shifted for TFX-*g*-PNIPAAm (133°C) and *net*-TFX-*g*-PNIPAAm (135°C), while these transitions were seen at 144 and 145°C for *IPN60D-c* and *s-IPN60D-c*, respectively. Both PNIPAAm and PAAc were included in the TFX bulk due to direct irradiation method applied; these results are consistent with the ESEM images.

Swelling Behavior and Temperature- and pH-Sensitiveness

Native TFX swelled up to 8–9% in buffer solution pH 7.0 at 25°C. For PNIPAAm grafted/crosslinked materials, swelling equilibrium (W_∞) was reached in <3 h, while for IPNs and *s*-IPNs the equilibrium was reached in 24 h. For example, *CGc-1step* reached the W_∞ level after about 1 h and its corresponding IPN (*IPNc-2steps*) at 24 h. The swelling degree increased as follows: TFX-*g*-PNIPAAm < *net*-TFX-*g*-PNIPAAm < *net*-TFX-*g*-PNIPAAm-*inter-net*-PAAc < TFX-*g*-PNI-

PAAm-*inter-net*-PAAc, except for *s-IPN80P* materials, which presented a high amount of extractable components (gel) under the conditions of swelling (Supporting Information Table SII). Most *s-IPNxP* polymers were swollen two times to remove excess gel and to achieve higher swelling degrees. The swelling degree increased with the grafting of PNIPAAm, its crosslinking and even more after interpenetration of PAAc network.

The LCST was between 21 and 26°C for TFX-*g*-PNIPAAm and *net*-TFX-*g*-PNIPAAm polymers (Figure 6, Supporting Information Table SII); namely various degrees below the LCST of pure PNIPAAm, in the range of 29–36°C.^{43,44} This suggests that the PNIPAAm chains associated to the aliphatic segments present in TFX. Oppositely, the LCST shifted to greater values (up to 32°C) when interpenetrated with PAAc probably because of the increase in hydrophilicity (Figure 6). The LCST and S_T values were generally higher in crosslinked polymers and its corresponding IPNs, as compared with grafted and *s*-IPNs materials. Crosslinking by γ -irradiation enhanced the difference between the swollen and collapsed state.

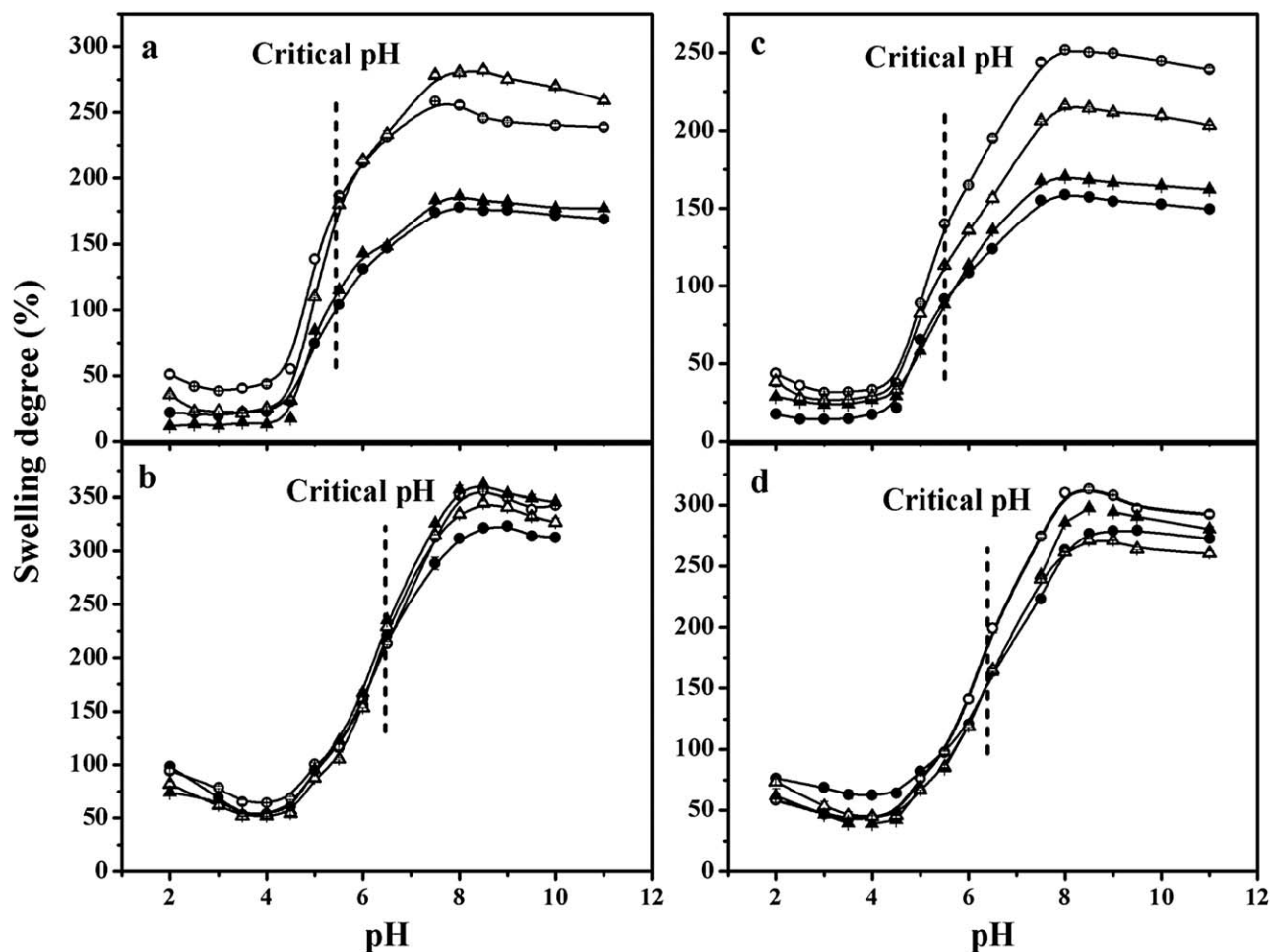


Figure 7. Swelling degree as a function of pH in buffer solutions, at 25°C, of TFX-*g*-PNIPAAm-*inter-net*-PAAc and *net*-TFX-*g*-PNIPAAm-*inter-net*-PAAc with PNIPAAm grafted by method P on catheters (a) and on films (c); and those with PNIPAAm grafted by method D on catheters (b) and films (d) for: IPN40 (●), *s*-IPN40 (○), IPN60 (▲) and *s*-IPN60 (△). The dashed line represents the critical points.

IPNxP and *s-IPNxP* exhibited pH-responsiveness with a critical pH in range of 5.1–5.7 while the critical pH of *IPNxD* and *s-IPNxD* was between 6.2 and 6.6 (Figure 7, Supporting Information Table SII). PAAc networks dispersed into the bulk matrix are less exposed to ionization of its carboxylic groups by action of the external pH than those interpenetrated onto polyurethane surface. Hydrogen bond formation and shorter distance among the acrylic acid groups caused the critical pH to shift from 5.1 to 6.6.^{22,24} S_{pH} increased with the amount of PNIPAAm/PAAc grafted on TFX. The *GCC-1step* showed LCST at 29°C while *IPN-2steps* behaved as dually responsive, being swollen at low temperature or alkaline pH, and collapse above 32°C or below pH 5.8 (Supporting Information Table SII).

Vancomycin Loading/Release and Antimicrobial Activity Test

Native TFX catheter and film only loaded small amount of vancomycin (ca. 12.7 mg/g). Grafting of IPNs and *s*-IPNs notably enhanced drug uptake (Figure 8). The amount of vancomycin loaded increased as the PNIPAAm/PAAc content rose. Although the loading was carried out for all polymers at 5°C, the total amount loaded was higher when preswollen polymers were directly placed into the drug solutions and the time required

for reaching equilibrium was lower (70 h), as compared with the dried polymers (~100 h). The *s*-IPNs also showed a somewhat enhanced loading compared to the IPNs probably because of a greater mesh size that facilitates the diffusion of the relative large glycopeptide antibiotic.

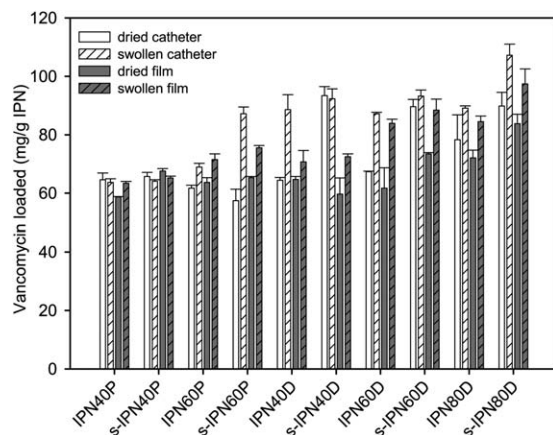


Figure 8. Capability of the IPNs grafted onto TFX catheters and films to load vancomycin.

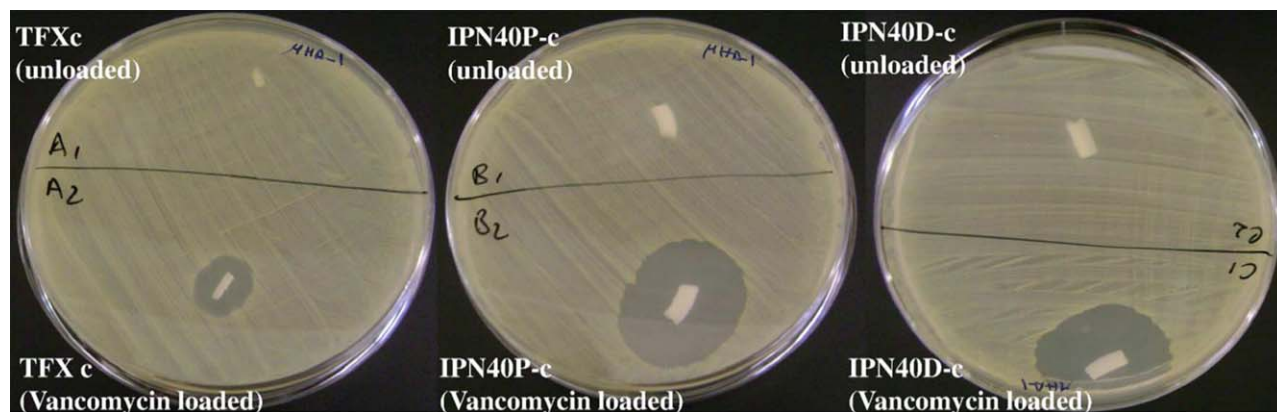


Figure 9. Zone inhibition of *Staphylococcus aureus* growth caused by native TFX catheter and IPN-grafted TFX catheter materials unloaded and loaded with vancomycin under sterile conditions. [Color figure can be viewed in the online issue, which is available at wileyonlinelibrary.com.]

DSC scans of vancomycin and drug-loaded *IPN40P-c* and *IPN40D-c* were recorded to gain an insight into the physical state of the drug in polymers. Vancomycin showed two endothermic transitions at 84 (T_{m1}) and 158°C (T_{m2}) [Supporting

Information Figure S4(a)].⁴⁵ Vancomycin-loaded *IPN40D-c* also showed the endothermic peak at 84°C and a broad transition corresponding to the melting point of polymer at 132°C [T_{mp} ; Supporting Information Figure S4(b)]. Conversely, drug-loaded

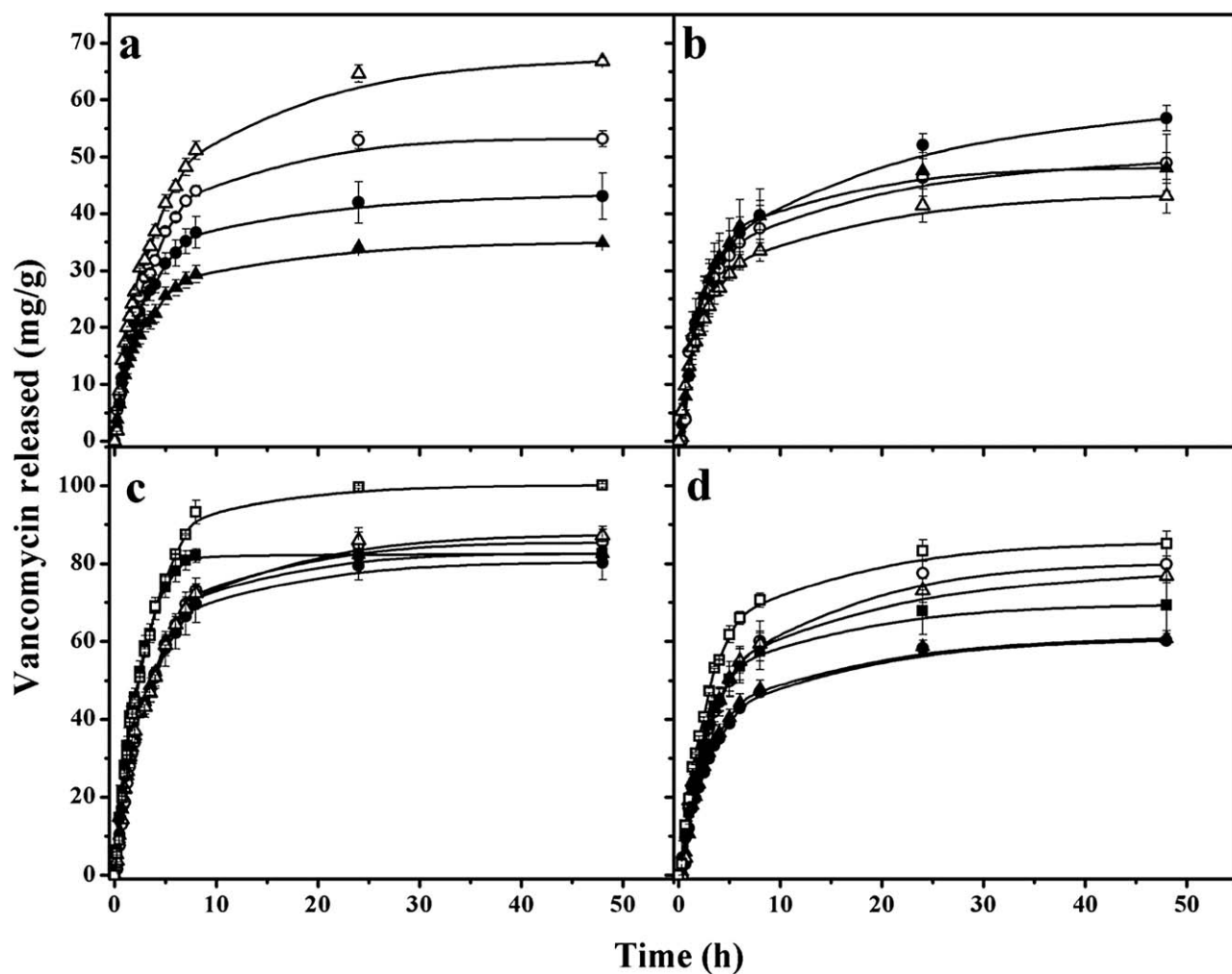


Figure 10. Vancomycin release profiles from *IPN40* (●), *s-IPN40* (○), *IPN60* (▲), *s-IPN60* (△), *IPN80* (■) and *s-IPN80* (□), in pH 7.4 phosphate buffers at 37°C for TFX catheter with PNIPAAm grafted via method P (a; b) and method D (c; d) from the swollen polymers (a; c) and previously dried materials.

IPN40P-c showed no endothermic transition at 84°C, but a transition with two minimum values at 128 (T_{mdp} , where dp indicates drug-polymer interaction) and 147°C (T_{mdp2}) was evidenced, indicating that there were changes on the crystalline phase of polymer [Supporting Information Figure S4(c)]. These results suggest that vancomycin would preferably be in a crystalline state in the *IPN40D-c*, while the drug would be in an amorphous state in *IPN40P-c* (dispersed into the polymer). The overlapping of peaks in *IPN40D-c* indicates that the two states (crystalline and amorphous) may be favored for the amount of drug loaded, but with a higher ratio of crystalline formations. Thus, interactions between the drug and the polymer are favored when the functionalization occurs on the polymer surface.

In vitro tests confirmed the capability of the vancomycin-loaded grafted polyurethanes to inhibit the growth of *S. aureus* (Figure 9, Supporting Information Table SIII). The inhibition zone diameters ranged from 20 to 30 mm. This antibacterial activity indicated that the release of vancomycin was above the MIC. Vancomycin release profiles obtained under sink conditions in phosphate buffer pH 7.4 at 37°C are shown in Figure 10. The IPNs-c and s-IPNs-c were able to sustain the release for more than 24 h. Similar results were found for *IPNc-2steps* and modified TFX films.

Protein Adsorption

Protein adsorption can influence platelet and endothelial cell adhesion on insertable devices and, thus, *in vitro* tests can anticipate to a certain extent the *in vivo* performance.^{46,47} Albumin adsorption may prevent platelet adhesion and the binding of microorganisms, while adsorption of IgG and fibrinogen favor adverse events promoting thrombus formation and microbial adhesion. The amounts of adsorbed albumin (BSA) and fibrinogen on unmodified and modified TFX film surfaces quantified applying the “amido black assay”⁴⁸ are shown in Figure 11(a). BSA concentration (30 mg/mL) was one order of magnitude greater than that of fibrinogen (3 mg/mL) to mimic the physiological levels.²⁹ Native TFX film sorbed more protein than the grafted materials, although less than nitrocellulose positive controls (1.4 mg fibrinogen/cm² ± 0.06 and 0.4 mg BSA/cm² ± 0.09). IPNs and s-IPNs predominantly sorbed BSA, compared to fibrinogen.

Hemolysis and Thrombogenicity

Erythrocytes were incubated in physiological buffer pH 7.4 in the presence of TFX catheter functionalized with PNIPAAm (*G40P-c*, *G40D-c*, *C40P-c*, and *C40D-c*) or PNIPAAm/PAAc (IPNs, s-IPNs and *IPNc-2steps*). In general, the hemolytic activity of materials was <5 %, including native TFX catheter with 3.1 % [Figure 11(b)]. *IPNc-2steps* was discarded for the following tests due to higher levels of hemolysis obtained, compared to other IPNs and s-IPNs. The *net*-TFXcatheter-*g*-PNIPAAm (*C40D-c*) obtained from PNIPAAm grafted in the bulk matrix by method D caused 4.8% hemolysis, while all IPNs and s-IPNs catheters showed levels between 1.1 and 3.2%. Crosslinking of PNIPAAm chains by γ -irradiation increased the hemolysis on the tested materials, while the incorporation of PAAc in the bulk of the polymer matrix did not cause any detrimental effect. These data confirm that the IPNs and s-IPNs are not hemolytic.

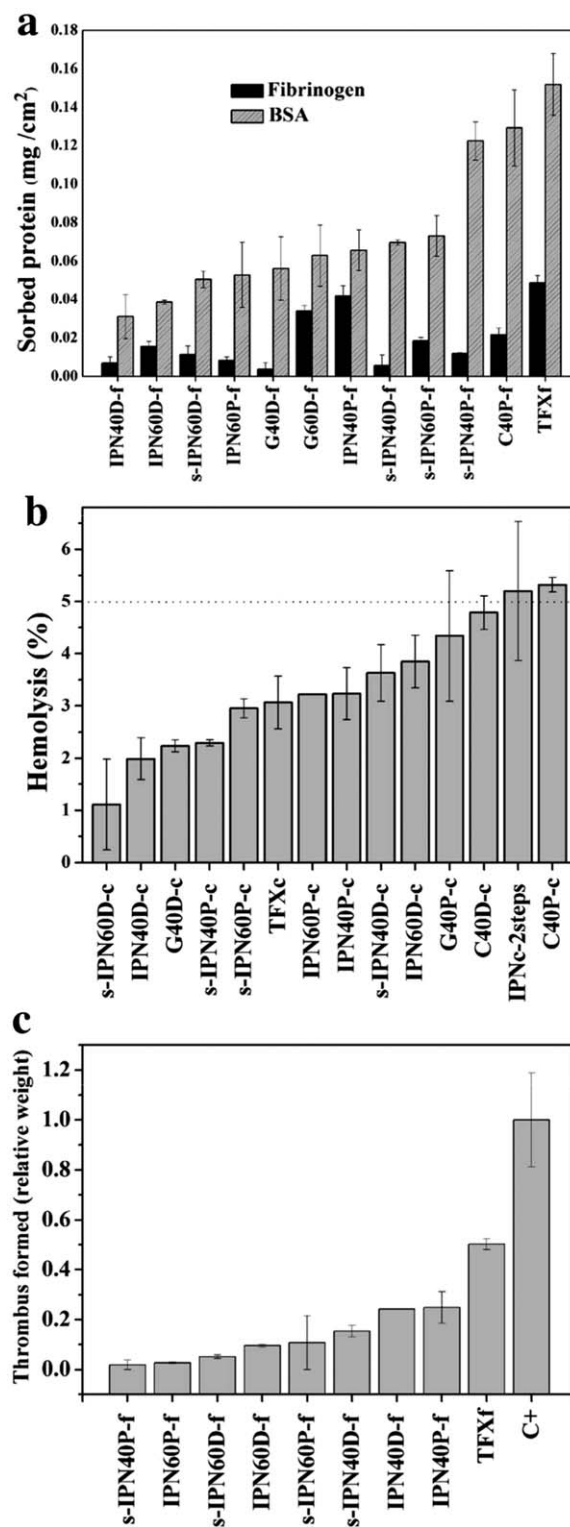


Figure 11. Adsorption of bovine serum albumin (BSA) and fibrinogen (a), percentage of hemolysis in rat blood (b), and thrombus formed after 30 min incubation (c) on native and modified TFX. The values of adsorption protein were given as a percentage of adsorption onto polymer surface. The dashed line in (b) corresponds to the permissible hemolysis level of 5%. The weight of thrombus formed on the surface-functionalized TFX film is normalized to that formed on control positive (C+). (The error bar is for standard deviation).

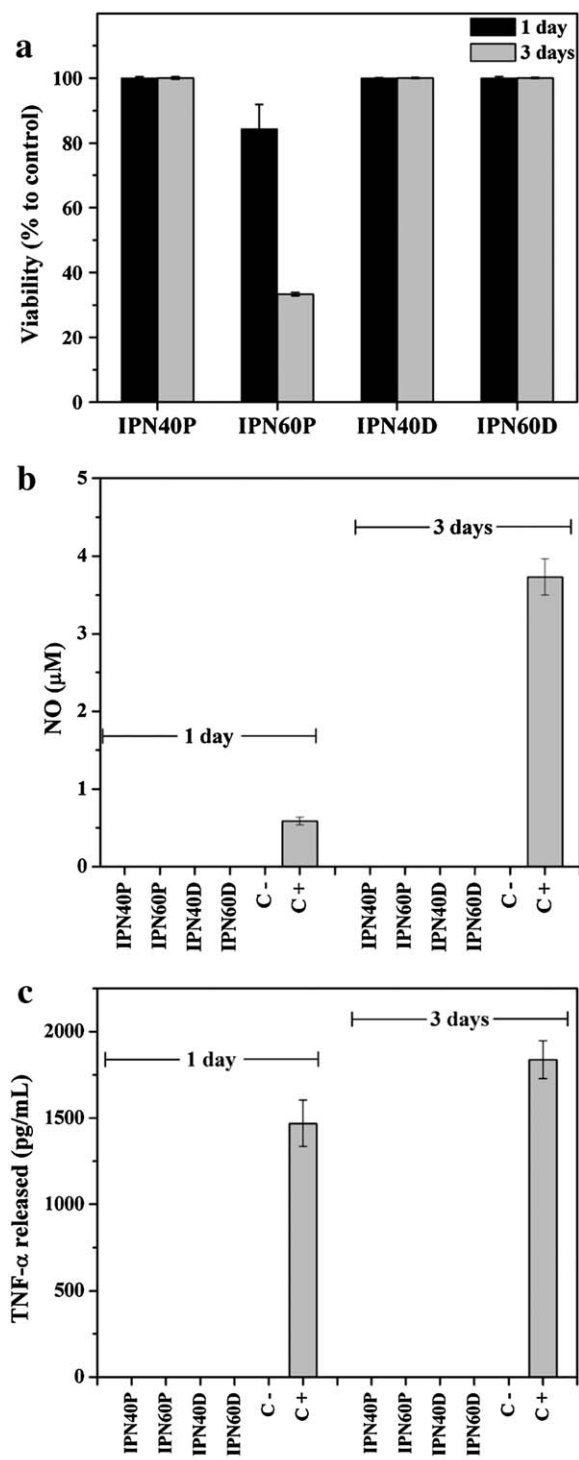


Figure 12. Viability (a), NO released (b) and TNF- α released (c) by RAW 264.7 macrophages (a), macrophages from 1 to 3 days, cultured over UV-irradiated IPNs. C- and C+ are negative and positive controls, respectively.

Thrombogenicity assays were performed on films in order to facilitate the quantification of thrombus by gravimetry after a contact time of 30 min. The glass Petri dish used as a positive control was highly thrombogenic ($0.044 \text{ g} \pm 0.008$) while native TFX film, commonly used as feedstock in the manufacture of

biomedical devices, was less thrombogenic ($0.022 \text{ g} \pm 0.001$). The relative weights of the clots formed on the surfaces of the modified TFX film were normalized to that formed on the positive control [Figure 11(c)]. All IPNs and s-IPNs were less thrombogenic than native TFX film, which confirmed the better blood compatibility of PNIPAAm/PAAc functionalized polyurethanes, as observed for other grafted materials.^{19,49}

Cytocompatibility

Cytocompatibility was tested using RAW 264.7 murine macrophages, which are highly sensitive to residual acrylate and methacrylate monomers.⁵⁰ Cell viability on each UV-sterilized IPNs was ca. 100% in the first 24 h [Figure 12(a)]. Some cells were cultured on the polymers loaded with vancomycin, and no toxic effects were observed either. The films showed cell viability values >50% at 3 days except for IPN60P-f, which presented extractable components (gel) under conditions of swelling. This factor negatively affected cell viability. Moreover, none of the IPNs seemed to activate cultured macrophages to produce NO [Figure 12(b)] and TNF- α [Figure 12(c)]. These results underscore the biocompatibility of test polymers.

CONCLUSIONS

Polyurethane Tecoflex[®] was functionalized via grafting/crosslinking of PNIPAAm/PAAc IPNs or s-IPNs by applying γ -ray irradiation in all steps of the synthesis, thus obtaining surface- or bulk-modified responsive TFX-based insertable medical devices able to load vancomycin and sustain its release. Compared with native TFX, the modification with IPNs and s-IPNs endows TFX with the ability to inhibit the growth of *S. aureus* acting as a drug delivery system, increases albumin adsorption and reduces fibrinogen adsorption, and improves the blood compatibility. Therefore, the approach implemented to modify polyurethane materials may well be useful to obtain drug-eluting insertable medical devices with minimized risk of infections.

ACKNOWLEDGMENTS

This work was supported by DGAPA-UNAM Grant IN202311, CONACYT-CNPq Project 174378 Mexico, MICINN (SAF2011-22771), Xunta de Galicia (PGIDT10CSA203013PR) Spain, FEDER, and the Ibero-American Programme for Science, Technology and Development of CYTED ("Red iberoamericana de nuevos materiales para el diseño de sistemas avanzados de liberación de fármacos en enfermedades de alto impacto socioeconómico" RIMADEL). The authors thank to Cristina Taboada and Ana Rey-Rico from USC for help with the blood and cell-compatibility tests.

REFERENCES

- Chen, K. Y., Kuo, J. F., Chen, C. Y. *Biomaterials* **2000**, *21*, 161–171.
- James, N. R., Philip, J., Jayakrishnan, A. *Biomaterials* **2006**, *27*, 160–166.
- Ulery, B. D., Nair, L. S., Laurencin, C. T. *J. Polym. Sci., Part B: Polym. Phys.* **2011**, *49*, 832–864.

4. Gottenbos, B., van der Mei, H. C., Busscher, H. J. *J. Biomed. Mater. Res., Part A* **2000**, *50*, 208–214.
5. Castner, D. G., Ratner, B. D. *Surf. Sci.* **2002**, *500*, 28–60.
6. Raad, I., Hanna, H., Maki, D. *Lancet Infect. Dis.* **2007**, *7*, 645–657.
7. Francois, P., Vaudaux, P., Nurdin, N., Mathieu, H. J., Descouts, P., Lew, D. P. *Biomaterials* **1996**, *17*, 667–678.
8. Khandwekar, A. P., Patil, D. P., Hardikar, A. A., Shouche, Y. S., Doble, M. *J. Biomed. Mater. Res., Part A* **2010**, *95A*, 413–423.
9. Borcan, F., Bolcu, C., Filimon, N., Bandur, G. *e-Polym.* **2012**, *80*, 1–8.
10. Sun, X., Cao, Z., Porteous, N., Sun, Y. *Acta Biomater.* **2012**, *8*, 1498–1506.
11. Park, D., Larson, A. M., Klibanov, A., Wang, Y. *Appl. Biochem. Biotechnol.* **2013**, *169*, 1134–1146.
12. Gnanasundaram, S., Ranganathan, M., Das, B. N., Mandal, A. B. *Colloids Surf., B* **2013**, *102*, 139–145.
13. Lv, W., Luo, J., Deng, Y., Sun, Y. *J. Biomed. Mater. Res., Part A* **2013**, *101A*, 447–445.
14. Clough, R.L. *Nucl. Instrum. Methods Phys. Res., Sect. B* **2001**, *185*, 8–33.
15. Hua, D., Cheng, K., Bai, W., Bai, R., Lu, W., Pan, C. *Macromolecules* **2005**, *38*, 3051–3053.
16. Zhou, X., Gao, W., Yang, H. *J. Mater. Sci.* **2006**, *41*, 3715–3722.
17. Alvarez-Lorenzo, C., Bucio, E., Burillo, G., Concheiro, A. *Expert Opin. Drug Delivery* **2010**, *7*, 173–183.
18. Kowalczyk, D., Ginalska, G., Golus, J. *Int. J. Pharm.* **2010**, *402*, 175–183.
19. Contreras-García, A., Alvarez-Lorenzo, C., Tobaoda, C., Concheiro, A., Bucio, E. *Acta Biomater.* **2011**, *7*, 996–1008.
20. Contreras-García, A., Bucio, E., Brackman, G., Coenye, T., Concheiro, A., Alvarez-Lorenzo, C. *Biofouling* **2011**, *27*, 123–135.
21. Ruiz, J. C., Burillo, G., Bucio, E. *Macromol. Mater. Eng.* **2007**, *292*, 1176–1188.
22. Ruiz, J. C., Alvarez-Lorenzo, C., Tobaoda, P., Burillo, G., Bucio, G., De Prijck, K., Nelis, H. J., Coenye, T., Concheiro, A. *Eur. J. Pharm. Biopharm.* **2008**, *70*, 467–477.
23. Muñoz-Muñoz, F., Ruiz, J. C., Alvarez-Lorenzo, C., Concheiro, A., Bucio, E. *Eur. Polym. J.* **2009**, *45*, 1859–1867.
24. Muñoz-Muñoz, F., Ruiz, J. C., Alvarez-Lorenzo, C., Concheiro, A., Bucio, E. *Radiat. Phys. Chem.* **2012**, *81*, 531–540.
25. Sperl, L. H.; Mishra, V. In *IPNs Around the World Science and Engineering*; Kim, S. C., Sperl, L. H., Eds.; John Wiley & Sons: New York, **1997**; Chapter 1, pp 1–25.
26. Perrin, D. D.; Dempsey, B. In *Buffers for pH and Metal Ion Control*. Chapman and Hall: London, **1994**, p 228.
27. Scott, C. P., Higham, P. A. *J. Biomed. Mater. Res., Part B* **2003**, *64*, 94–98.
28. Dieckmann-Schuppert, A., Schnittler, H. *J. Cell Tissue Res.* **1997**, *288*, 119–126.
29. Zha, Z., Ma, Y., Yue, X., Liu, M., Dai, Z. *Appl. Surf. Sci.* **2009**, *256*, 805–814.
30. Imai, Y., Nose, Y. *J. Biomed. Mater. Res.* **1972**, *6*, 165–172.
31. Saad, B., Keiser, O. M., Uhlschmid, G. K., Marquardt, K., Welti, M., Neuenschwander, P., Suter, U. W. *J. Mater. Sci.: Mater. Med.* **1997**, *8*, 497–505.
32. Ding, A. H., Nathan, C. F., Stuehr, D. J. *J. Immunol.* **1988**, *141*, 2407–2414.
33. Mizumoto, D., Nojiri, C., Inomata, Y., Onishi, M., Waki, M., Kido, T., Sugiyama, T., Senshu, K., Uchida, K., Sakai, K., Akutsu, T. *ASAIO J.* **1997**, *43*, M500–M504.
34. Bucio, E., Burillo, G., Adem, E., Coqueret, X. *Macromol. Mater. Eng.* **2005**, *290*, 745–752.
35. Guignot, C., Betz, N., Legendre, B., Le Moel, A., Yagoubi, N. *Nucl. Instrum. Methods Phys. Res., Sect. B* **2001**, *185*, 100–107.
36. Khandwekar, A. P., Doble, M. *J. Mater. Sci.: Mater. Med.* **2011**, *22*, 1231–1246.
37. Schmidt, C., Chowdhury, A. M., Neuking, K., Eggeler, G. *J. Polym. Res.* **2011**, *18*, 1807–1812.
38. Tu, H., Heitzman, C. E., Braun, P. V. *Langmuir* **2004**, *20*, 8313–8320.
39. Gomez-Carracedo, A., Alvarez-Lorenzo, C., Gomez-Amoza, J. L., Concheiro, A. *Int. J. Pharm.* **2004**, *274*, 233–243.
40. Schmidt, C., Neuking, K., Eggeler, G. *Mater. Res. Soc. Symp. Proc.* **2009**, *1190*, 43–48.
41. Koberstein, J., Leung, L. *Macromolecules* **1992**, *23*, 6205–6213.
42. Menczel, J. D.; Prime, R. B. In *Thermal analysis of polymers. Fundamentals and applications*; John Wiley & sons: Chichester, **2009**; p 7.
43. Hirokawa, Y., Tanaka, T. *J. Chem. Phys.* **1984**, *181*, 6379–6380.
44. Schild, H. G. *Prog. Polym. Sci.* **1992**, *17*, 163–249.
45. Loveymi, B. D., Jelvehgari, M., Zakeri-Milani, P., Valizadeh, H. *Adv. Pharm. Bull.* **2012**, *2*, 43–56.
46. Lindon, J. N., McManama, G., Kushner, L., Merrill, E. W., Salzman, E. W. *Blood* **1986**, *68*, 355–362.
47. Bernacca, G. M., Gulbransen, M. J., Wilkinson, R., Wheatley, D. J. *Biomaterials* **1998**, *19*, 1151–1165.
48. Heinzl, W., Vogt, A., Kallee, E., Faller, W. *J. Lab. Clin. Med.* **1965**, *66*, 334–343.
49. Sugiyama, K., Matsumoto, T., Yamazaki, Y. *Macromol. Mater. Eng.* **2000**, *282*, 5–12.
50. Lin, N. J., Bailey, L. O., Becker, M. L., Washburn, N. R., Henderson, L. A. *Acta Biomater.* **2007**, *3*, 163–173.